Full Waveform seismic AVAZ responses from orthorhombic model

Sitamai W. Ajiduah
Gary F. Margrave

Banff, AB @ 2017

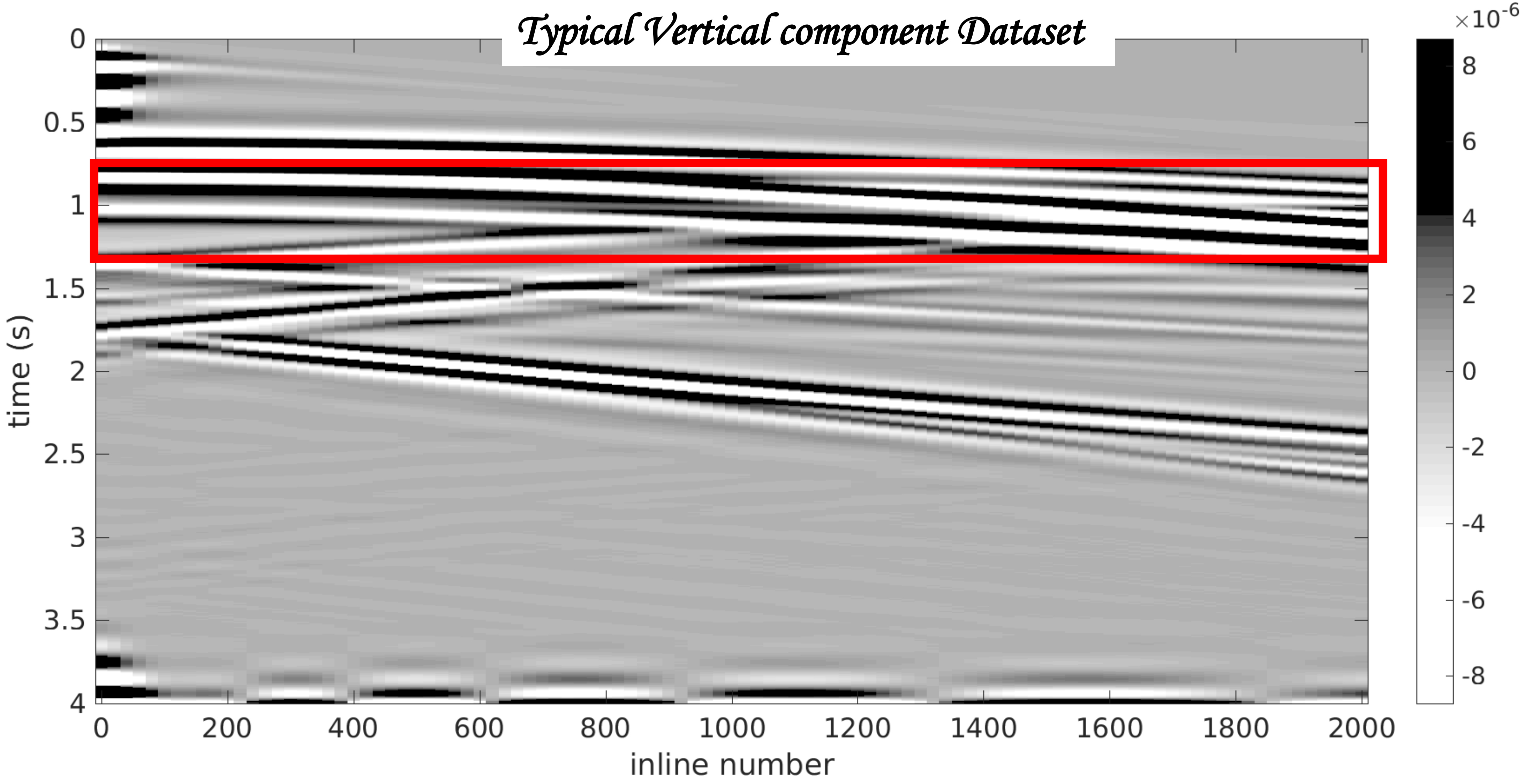
Typical Vertical component Dataset
time (s)
inline number
0
0.5
1
1.5
2
2.5
3
3.5
4
0
200
400
600
800
1000
1200
1400
1600
1800
2000
×10^-6
8
6
4
2
0
-2
-4
-6
-8

Typical Radial component Dataset

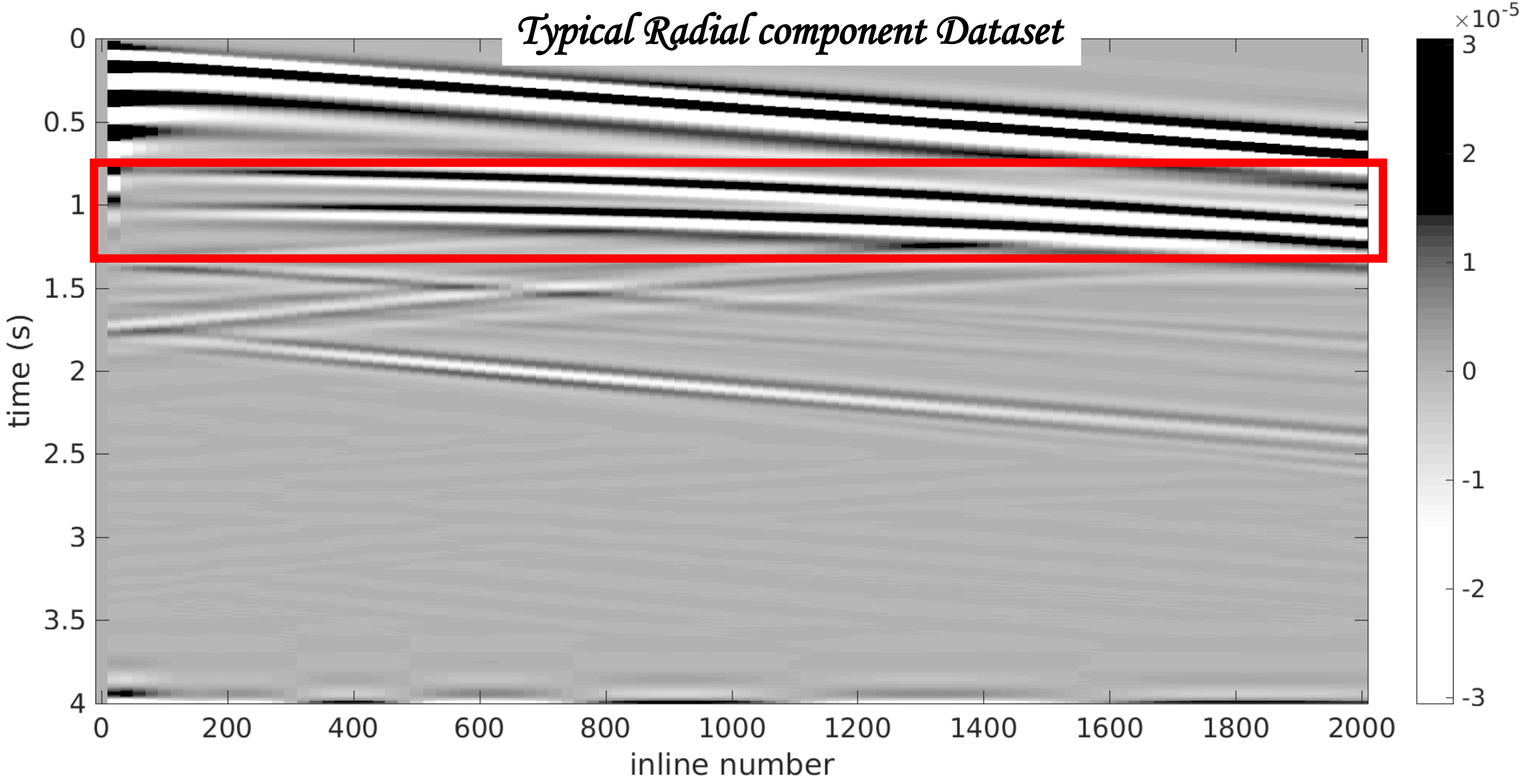

Typical Transverse-component Dataset

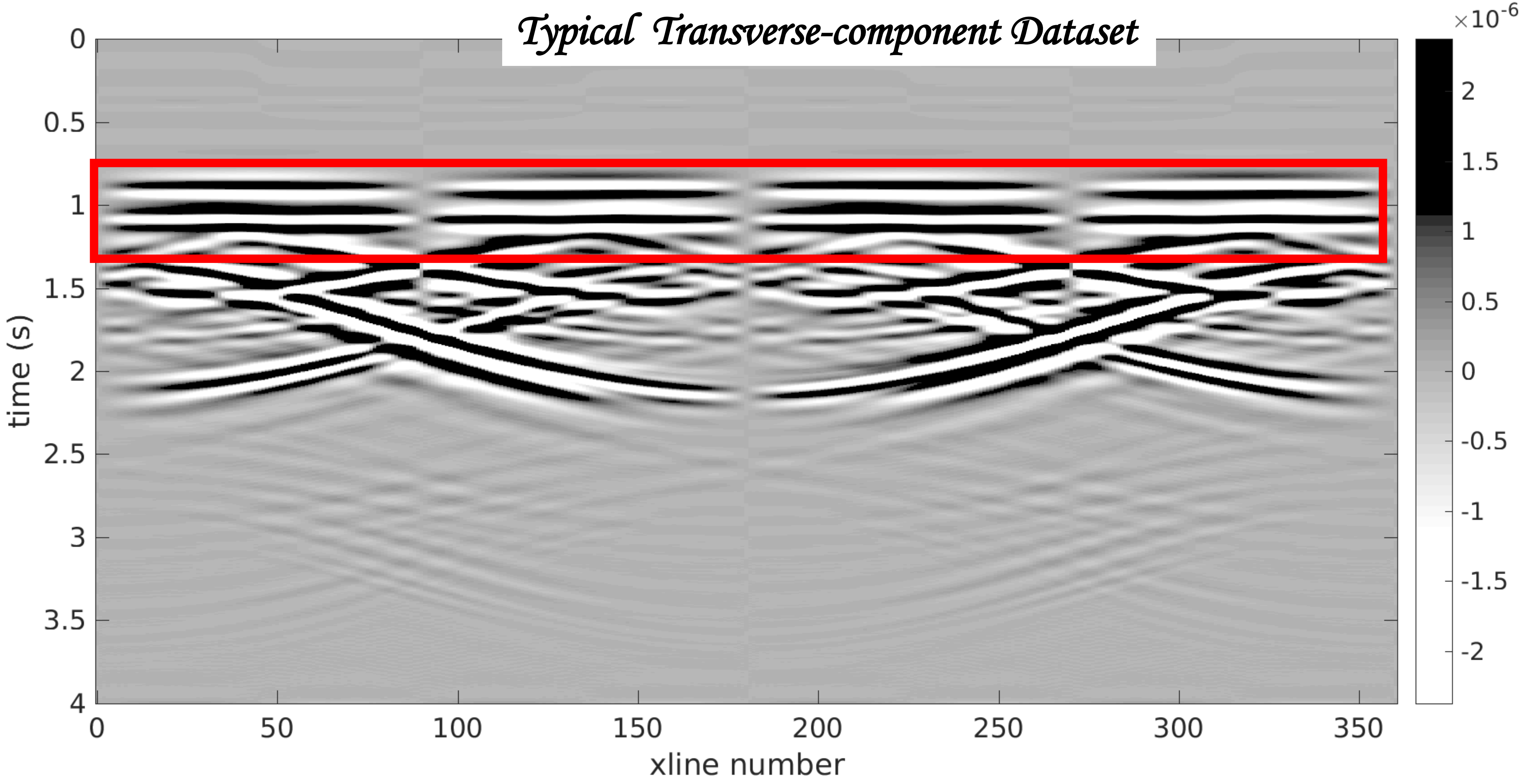

- ❑ *Introduction*
- ❑ *Analogy between VTI HTI & ORT*
- ❑ *Review of Azimuthal AVO analysis*
- ❑ *Numerical Examples*
- ❑ *Conclusion*
- ❑ *Acknowledgements*

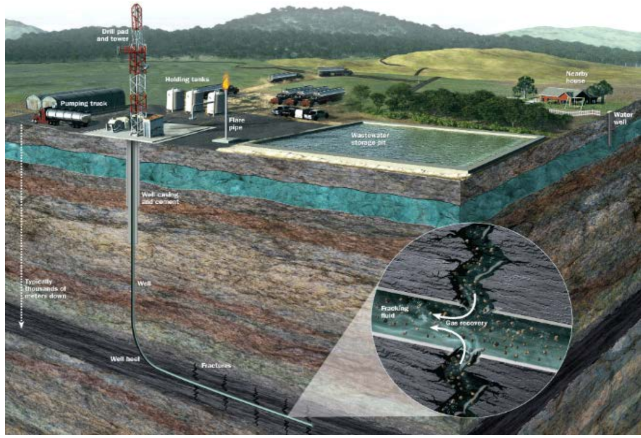

- *Simple subsurface models like VTI HTI and Orthorhombic model are important tools in subsurface fracture studies.*
- *Studies have also shown that AVOaz fracture behavior is effective for seismic characterization of fractures.*
- *Aim to gain insight into fracture behaviour of orthorhombic anisotropy*

❖ *Analogy between VTI HTI & ORT*

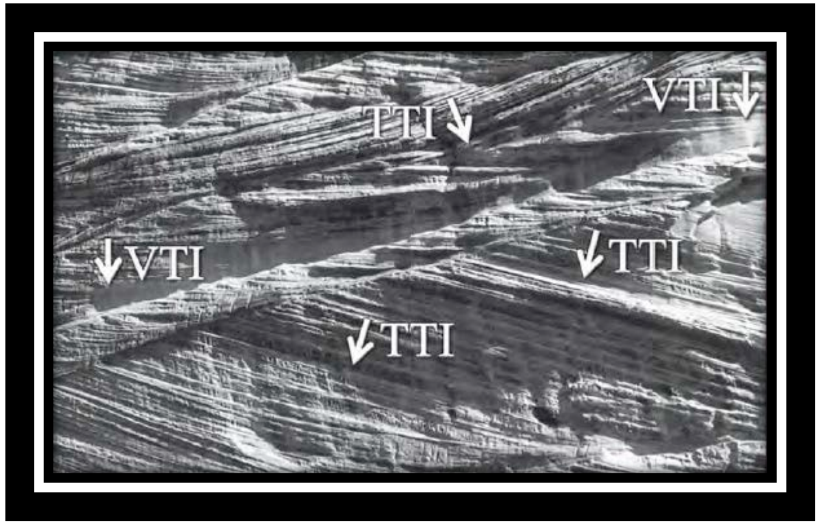

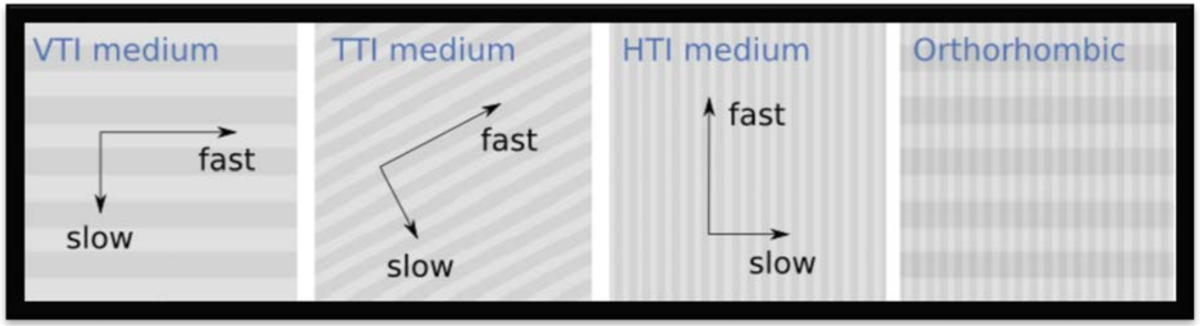

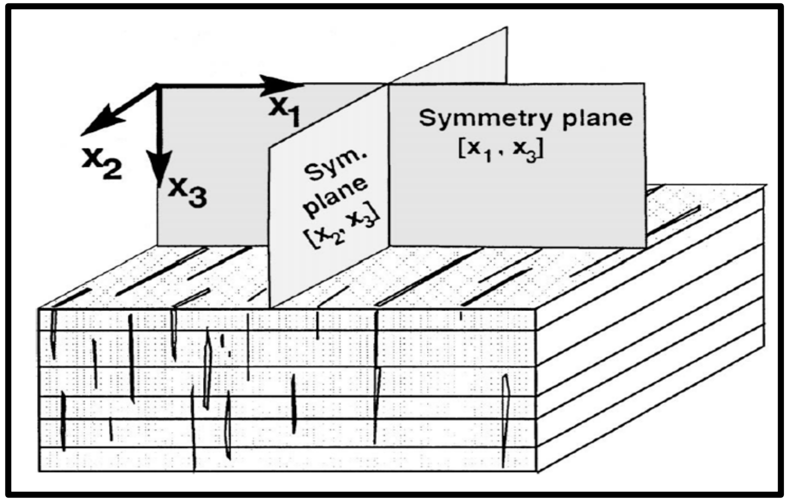

Symmetry planes in orthorhombic media where anisotropy after Tsvankin, (2001).

Typical orthorhombic modeling of shale reservoir requires at least a VTI/HTI, VTI/TTI, HTI/HTI or a VTI/Orthorhombic models.

Review of Azimuthal AVO analysis

➢ *equivalence between the symmetry planes of TI and orthorhombic models*

$$R^{VTI} = \frac{1}{2}\frac{\Delta Z}{\bar{Z}} + \frac{1}{2}\left[\frac{\Delta\alpha_0}{\bar{\alpha}_0} - \left(\frac{2\bar{\beta}_0}{\bar{\alpha}_0}\right)^2 \frac{\Delta G}{\bar{G}} + \Delta\delta\right] sin^2 i + \frac{1}{2}\left[\frac{\Delta\alpha_0}{\bar{\alpha}_0} + \Delta\epsilon\right] sin^2 i\, tan^2 i$$

$$R^{[x_2-x_3]} = \frac{1}{2}\frac{\Delta Z}{\bar{Z}} + \frac{1}{2}\left[\frac{\Delta\alpha_0}{\bar{\alpha}_0} - \left(\frac{2\bar{\beta}_0}{\bar{\alpha}_0}\right)^2 \frac{\Delta G}{\bar{G}} + \Delta\delta^{(1)}\right] sin^2 i + \frac{1}{2}\left[\frac{\Delta\alpha_0}{\bar{\alpha}_0} + \Delta\epsilon^{(1)}\right] sin^2 i\, tan^2 i$$

$$R^{[x_1-x_3]} = \frac{1}{2}\frac{\Delta Z}{\bar{Z}} + \frac{1}{2}\left[\frac{\Delta\alpha_0}{\bar{\alpha}_0} - \left(\frac{2\bar{\beta}_0}{\bar{\alpha}_0}\right)^2 \left(\frac{\Delta G}{\bar{G}} + \Delta\gamma^S\right) + \Delta\delta^{(2)}\right] sin^2 i + \frac{1}{2}\left[\frac{\Delta\alpha_0}{\bar{\alpha}_0} + \Delta\epsilon^{(2)}\right] sin^2 i\, tan^2 i$$

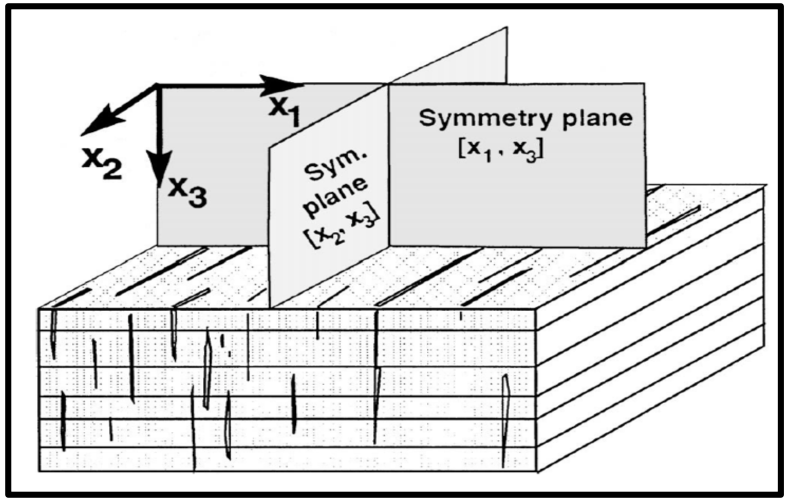

Symmetry planes in orthorhombic media where anisotropy after Tsvankin, (2001).

Review of Azimuthal AVO analysis

- Reflection coefficient between symmetry planes

$$R^{[x_1-x_3]} - R^{[x_2-x_3]} = \left[\left(\frac{2\bar{\beta}_0}{\bar{a}_0}\right)^2 \Delta\gamma^S + \frac{1}{2}\left(\Delta\delta^{(2)} - \Delta\delta^{(1)}\right)\right] sin^2 i. + \frac{1}{2}\left[\Delta\epsilon^{(2)} - \Delta\epsilon^{(1)}\right] sin^2 i tan^2 i$$

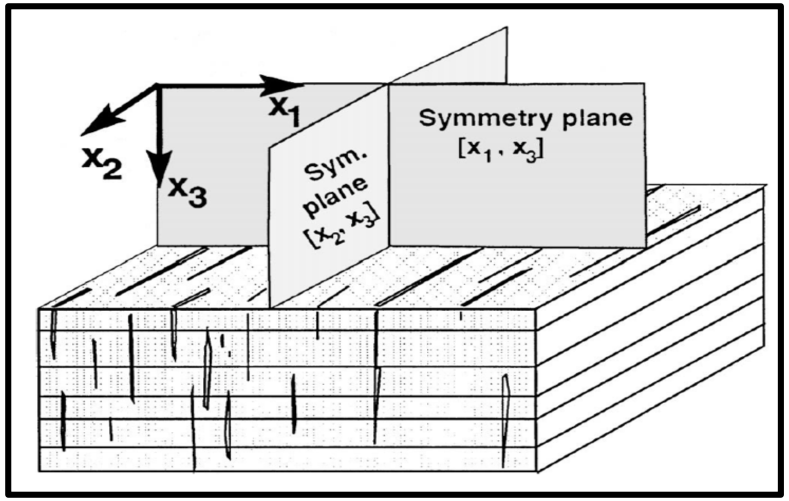

Symmetry planes in orthorhombic media where anisotropy after Tsvankin, (2001).

- If Incidence medium is isotropic, $\Delta\gamma^S$ and the differences becomes

$$R^{[x_1-x_3]} - R^{[x_2-x_3]} = \left[\left(\frac{2\bar{\beta}_0}{\bar{a}_0}\right)^2 \gamma^S + \frac{1}{2}\left(\delta^{(2)} - \delta^{(1)}\right)\right] sin^2 i. + \frac{1}{2}\left[\epsilon^{(2)} - \epsilon^{(1)}\right] sin^2 i tan^2 i$$

Review of Azimuthal AVO analysis

- *Azimuthal Variation of AVO Gradient*

- $B_{PP}^{ani} = B_{PP}^{\perp} + B_{PP}^{\parallel}$

For isotropic/Orthorhombic Interface

- $B_{PP}^{ani} = \frac{(\delta^{(2)} - \delta^{(1)}) - 8g\gamma^{S}}{2}$

- $g \equiv \bar{\beta}_0 / \bar{\alpha}_0$
- *If g approaches 0.25* $\Longrightarrow B_{PP}^{ani} = \frac{1}{2}(\delta^{(2)} - \delta^{(1)}) - \gamma^{S}$
- $(\delta(2) - \delta(1))$ *controls the eccentricity of the P-wave NMO ellipse*

- *Detailed analysis of mode-converted waves in anisotropic media, Jilek (2002b).*

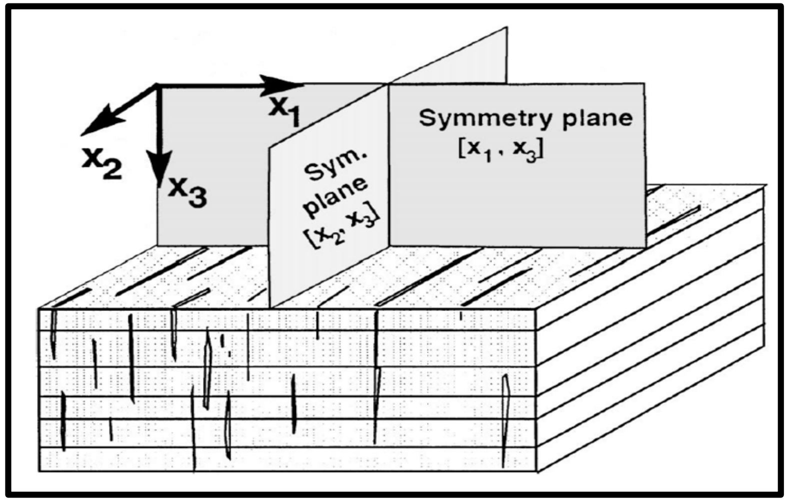

Symmetry planes in orthorhombic media where anisotropy after Tsvankin, (2001).

❖ *Plan view and model parameters*

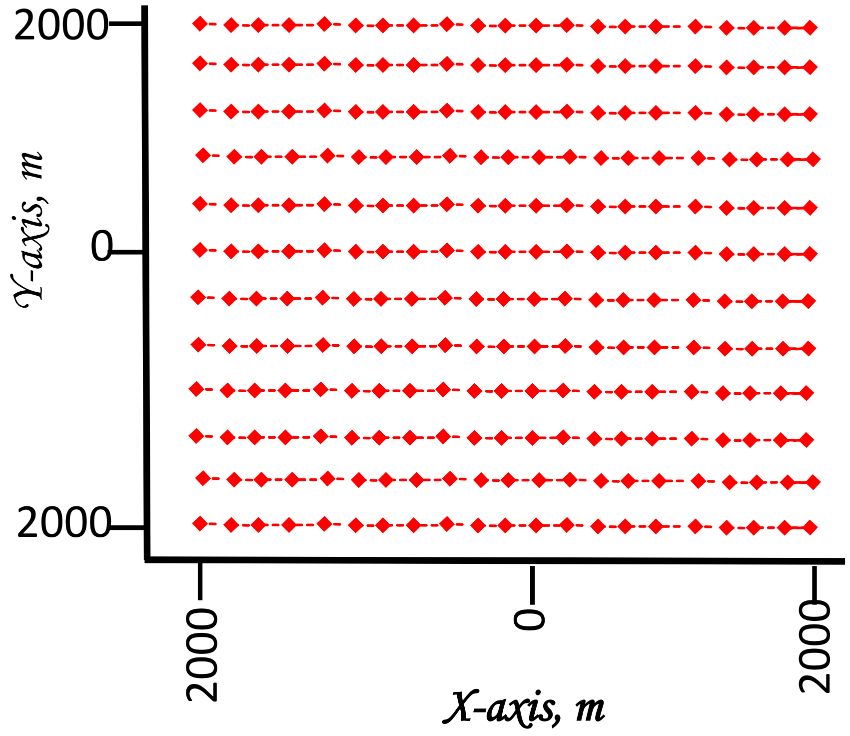

Scheme:	*elastic*
Source representation:	*Moment density tensor.*
Source type:	*Vertical displacement type of 15Hz*
No of Shots:	*1*
No of Receiver:	*40401*
Grid dimension:	*201 x 201 x 201*
Grid spacing:	*20*
Min Vel. and non-zero Vs):	*2230m/s*
Min wavelength:	*148.m (8 times the average thick)*
Top boundary thickness:	*659 cells*
Bottom boundary thickness:	*698 cells*
Left/right boundary thickness:	*689 cells*
Maximum p-wave velocity:	*5039.957 m/s,*
Courant factor:	*0.85,*
Temporary sampling in FD modeling:	*0.0013631727*

❖ *Stiffness matrix of HTI and Orthorhombic*

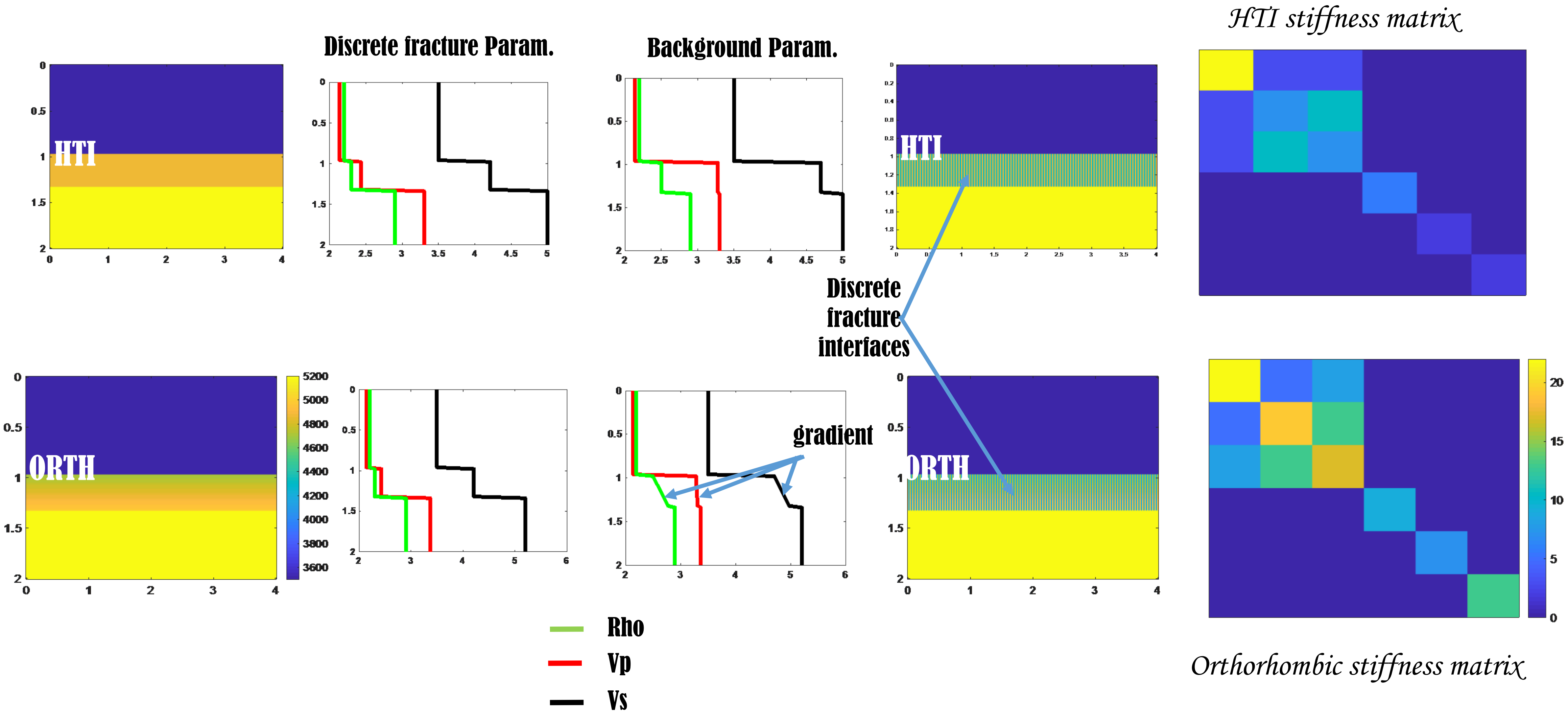

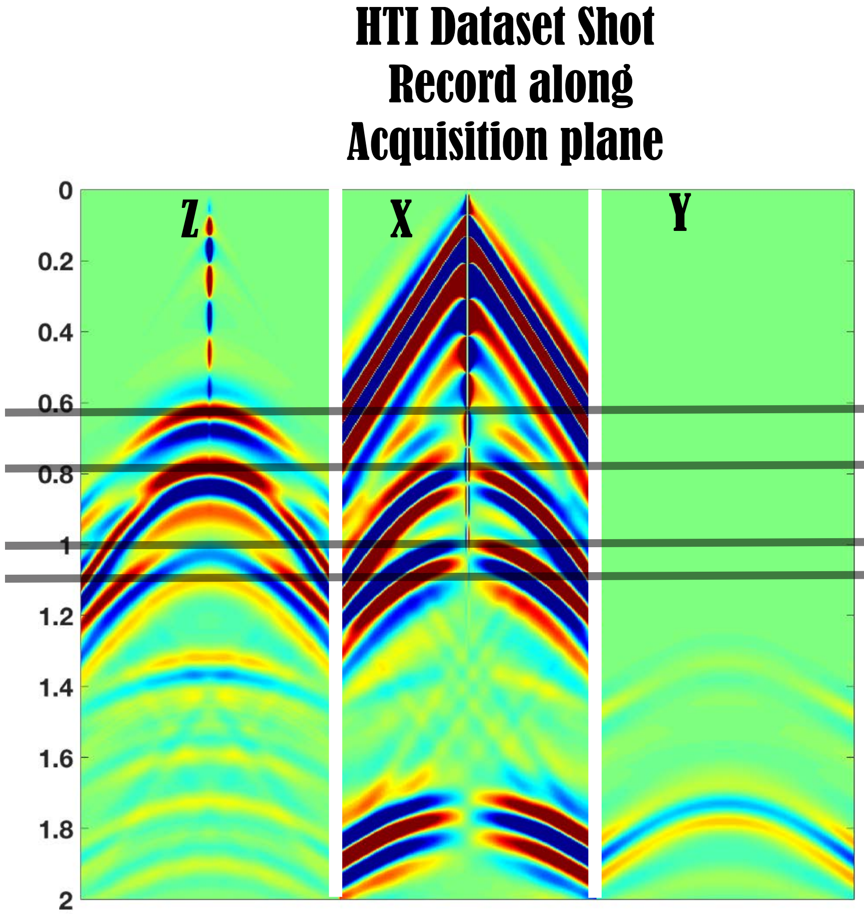
HTI Dataset Shot Record along Acquisition plane
Z
X
Y
0
0.2
0.4
0.6
0.8
1
1.2
1.4
1.6
1.8
2

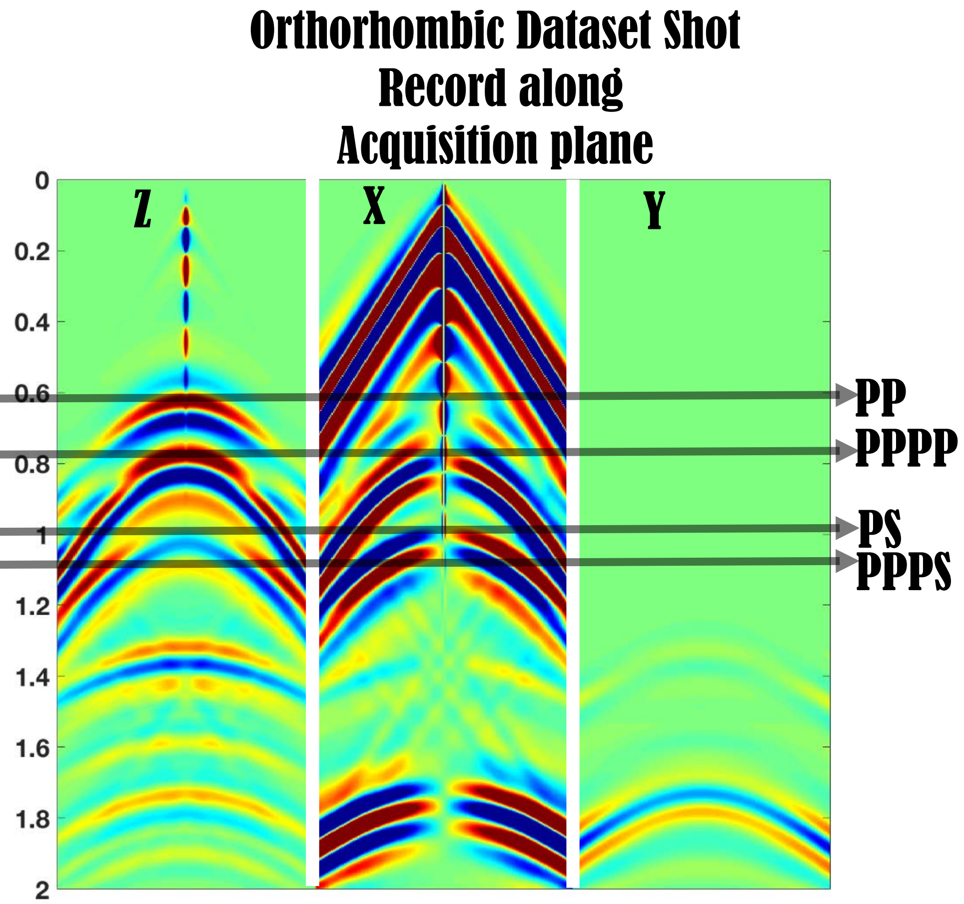
Orthorhombic Dataset Shot Record along Acquisition plane
Z
X
Y
0
0.2
0.4
0.6
0.8
1
1.2
1.4
1.6
1.8
2
PP
PPPP
PS
PPPS

HTI Common Azimuth Dataset along Symmetry plane

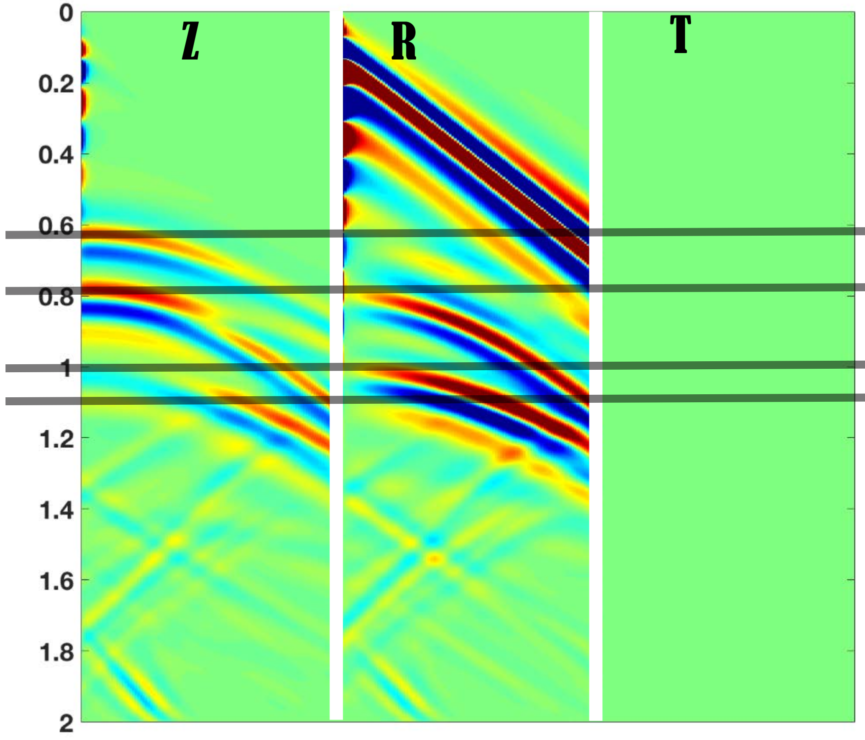

Orthorhombic Common Azimuth Dataset along Symmetry plane

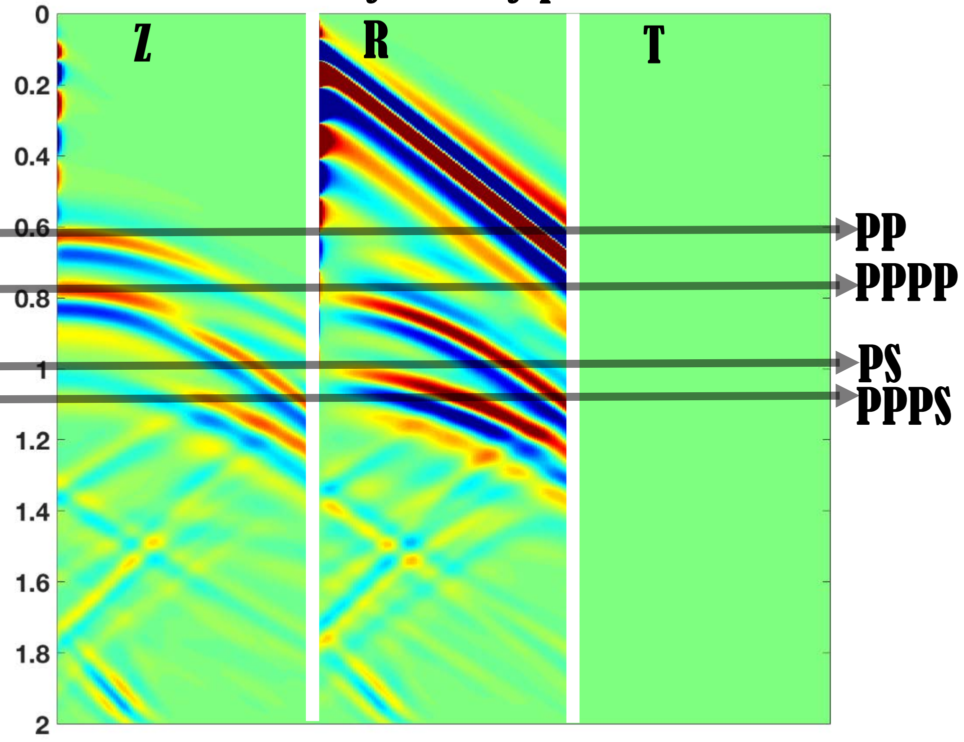

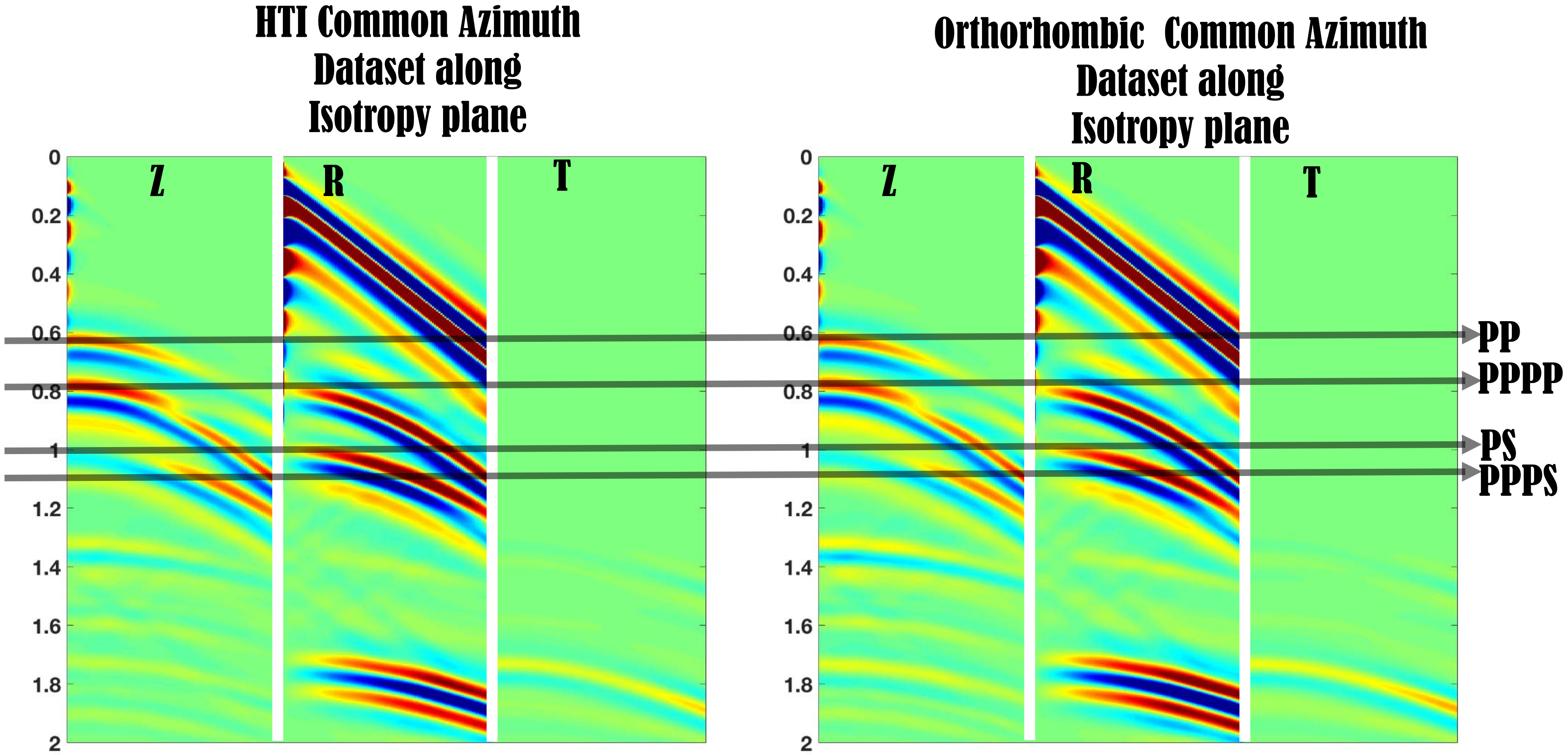

HTI Common Azimuth
Dataset along
Isotropy plane
Orthorhombic Common Azimuth
Dataset along
Isotropy plane
Z
R
T
0
0.2
0.4
0.6
0.8
1
1.2
1.4
1.6
1.8
2
PP
PPPP
PS
PPPS

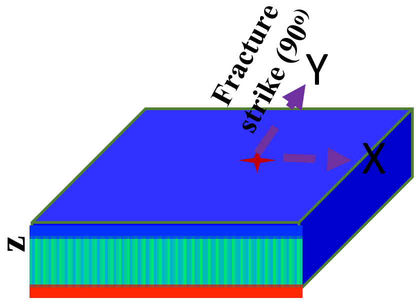

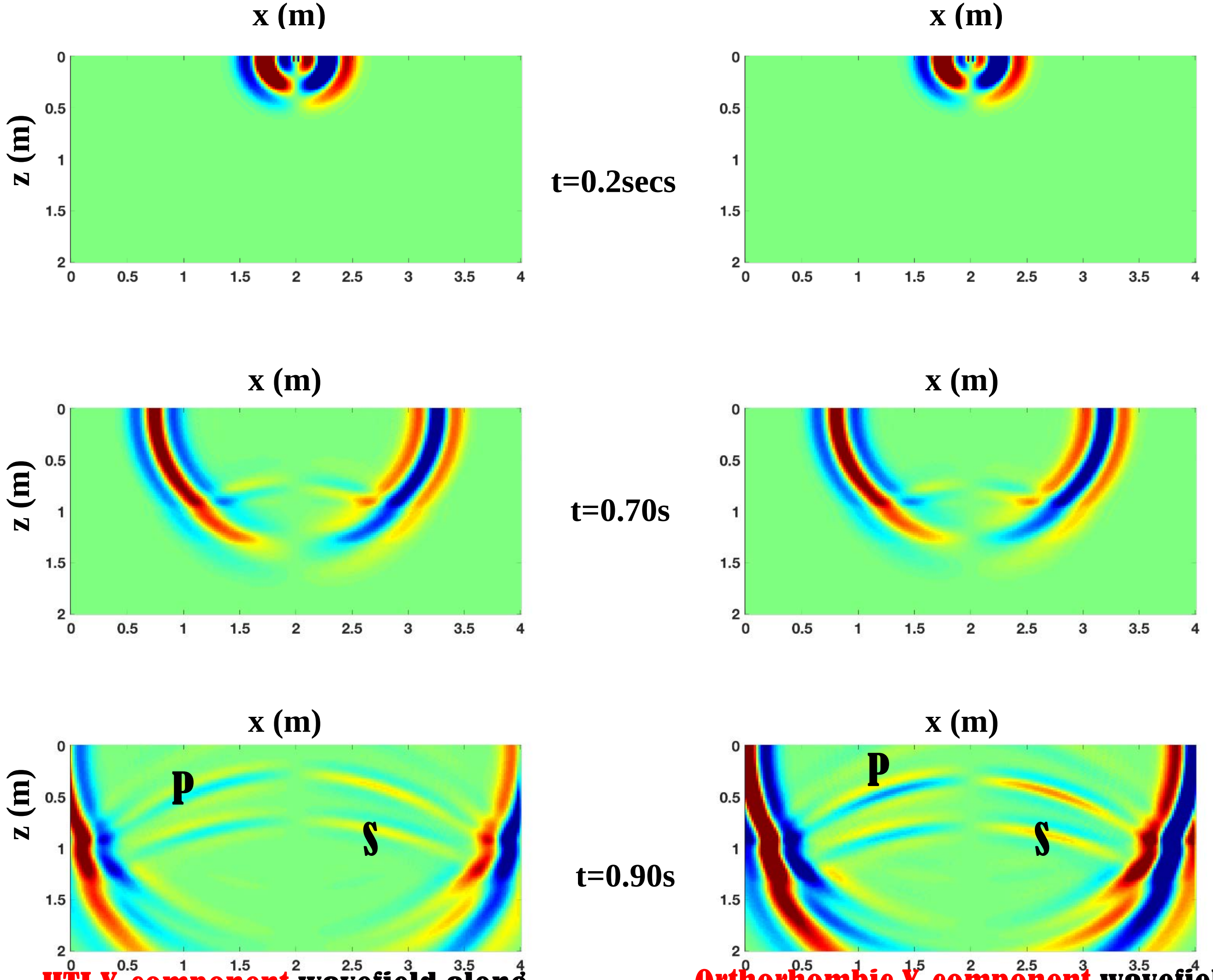

HTI X-component wavefield along isotopy plane

Orthorhombic X-component wavefield along isotopy plane

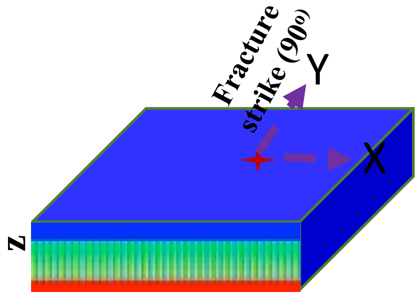

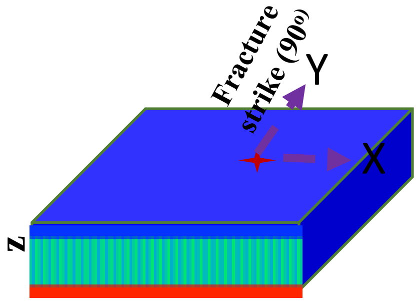

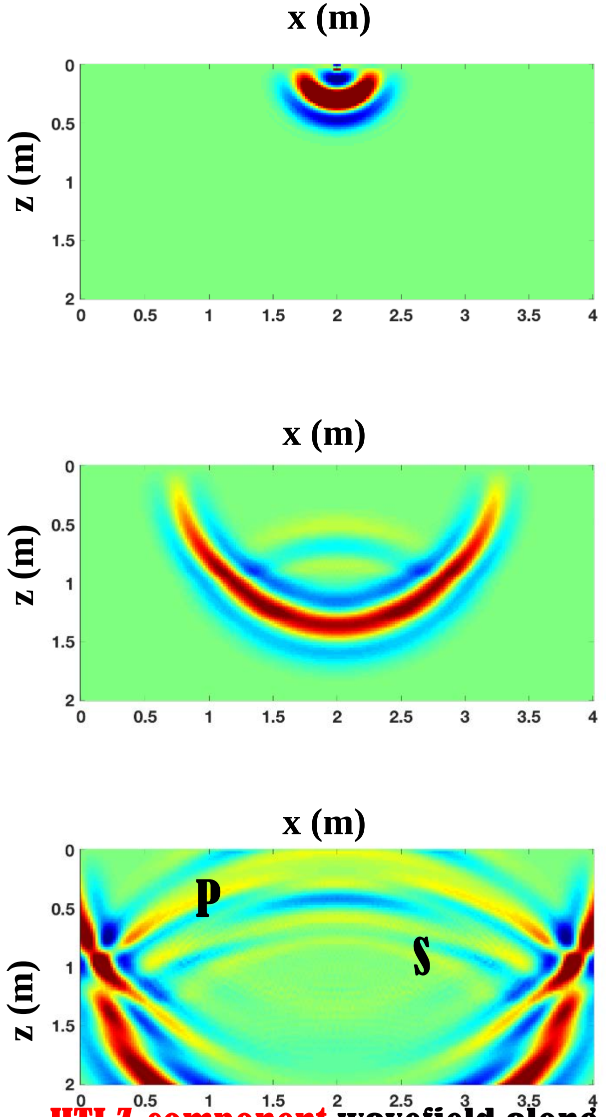

t=0.2secs

t=0.70s

t=0.90s

HTI Z-component wavefield along isotopy plane

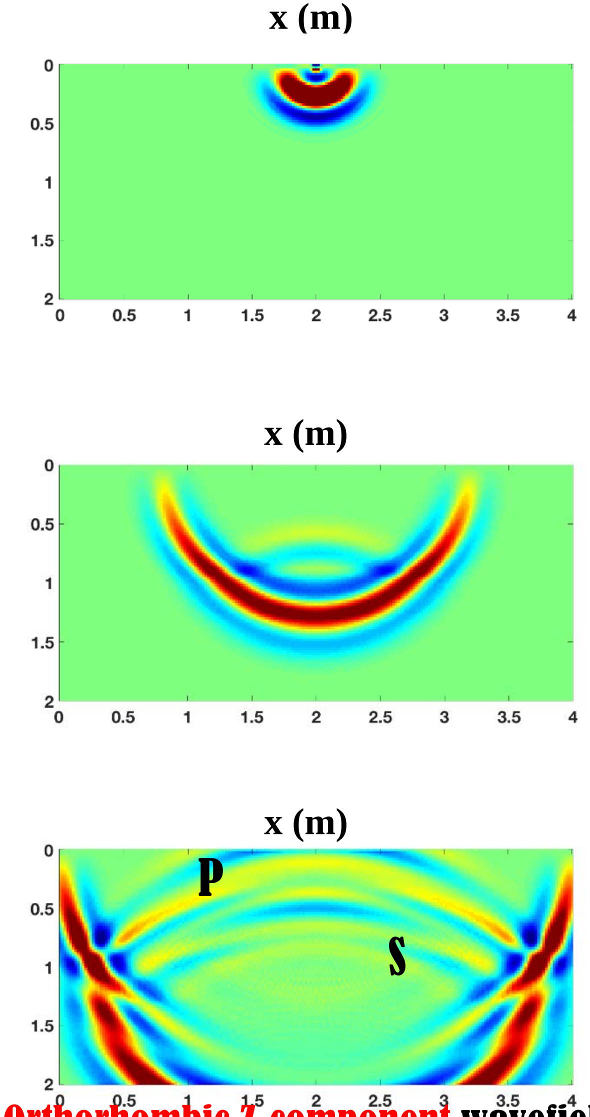

Orthorhombic Z-component wavefield along isotopy plane

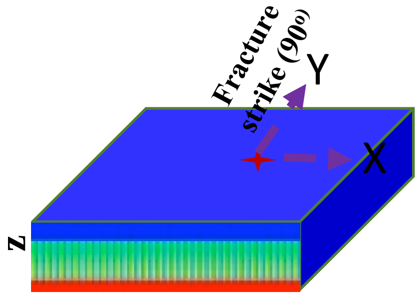

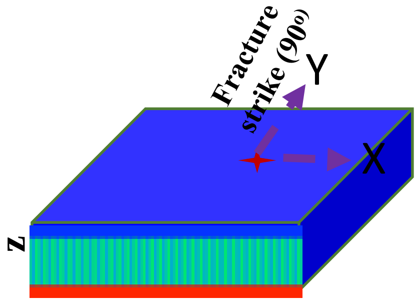

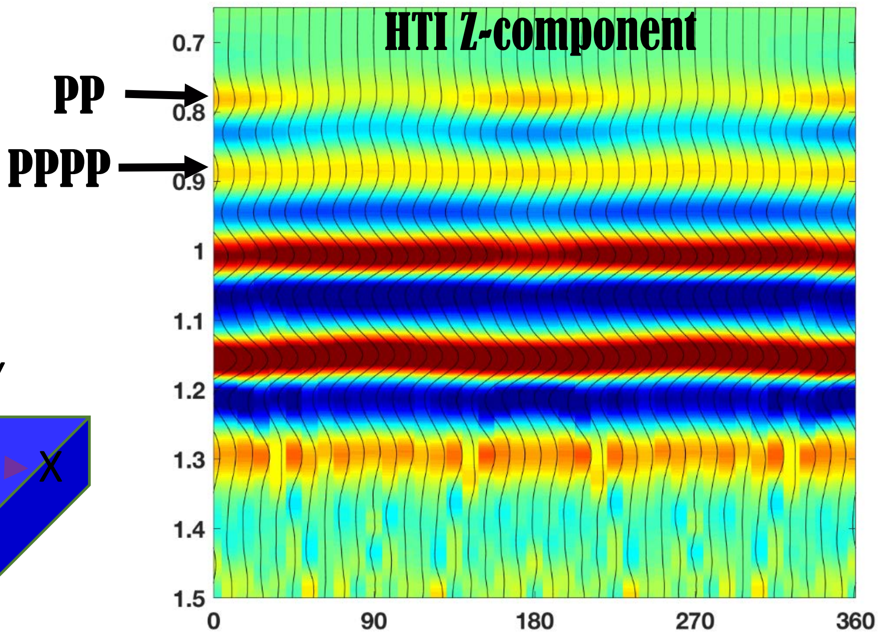

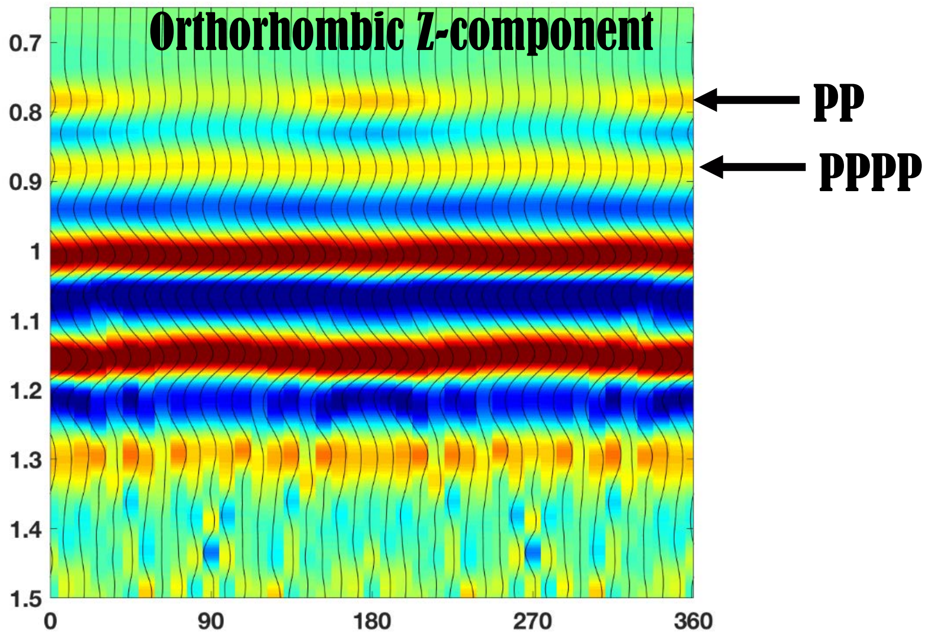

VTI background has no effect on PP reflections.

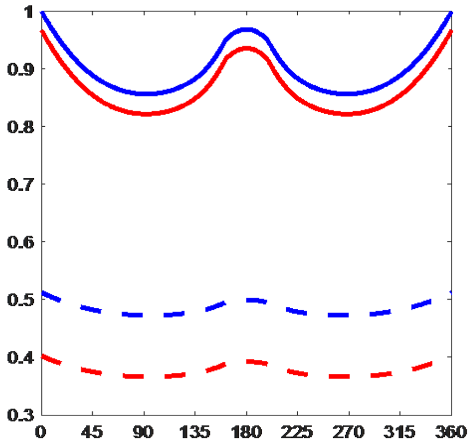

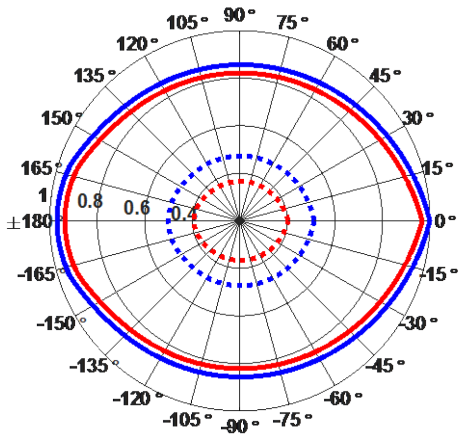

legend
- PP HTI Refl. from top
- PPPP HTI Refl. from bottom
- PP Ortho. Refl. from top
- PPPP Ortho. Refl. from bottom

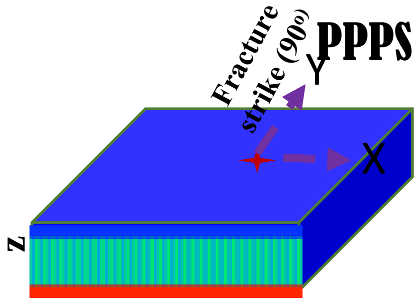

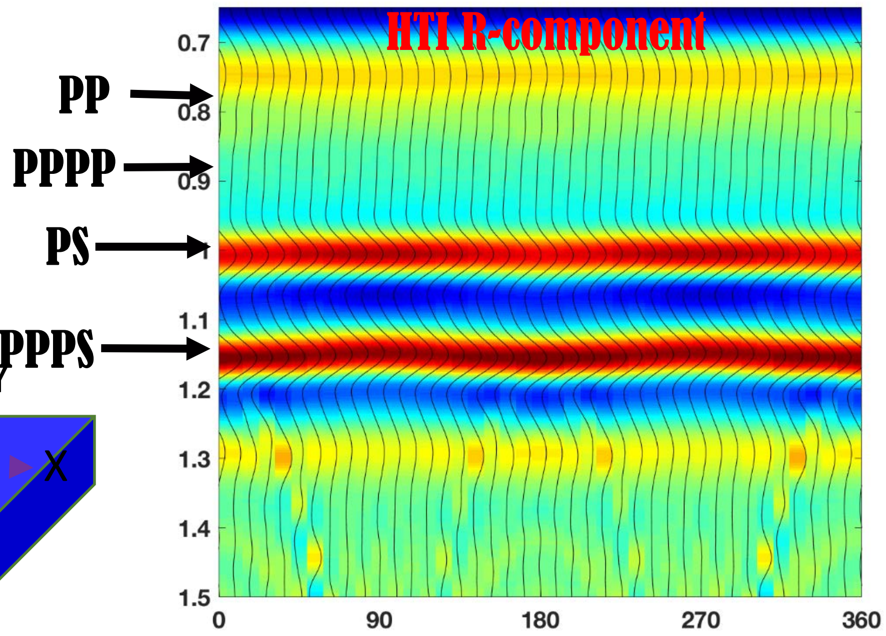

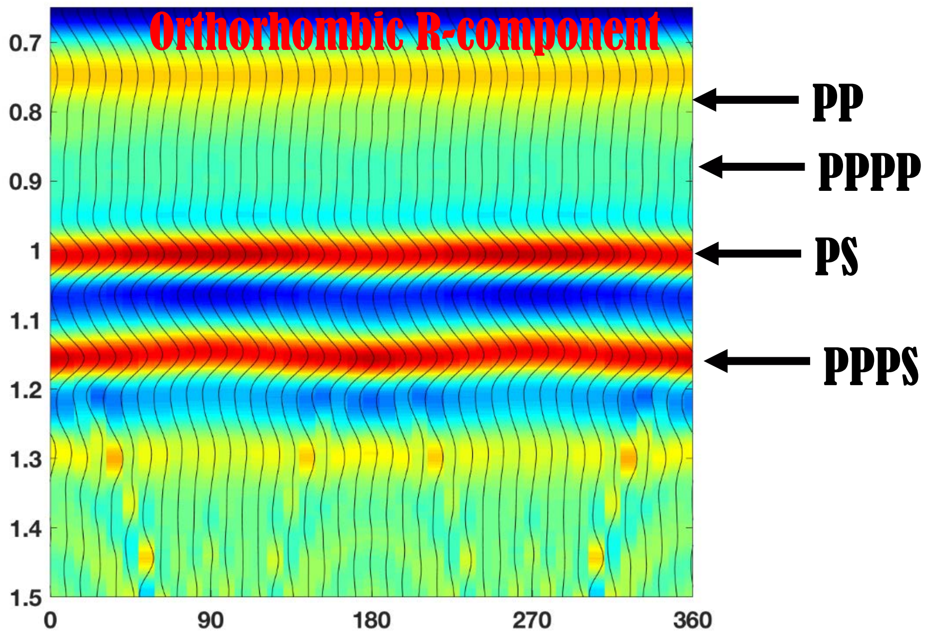

The VTI background rotates the fracture orientation estimation by 90 degrees.

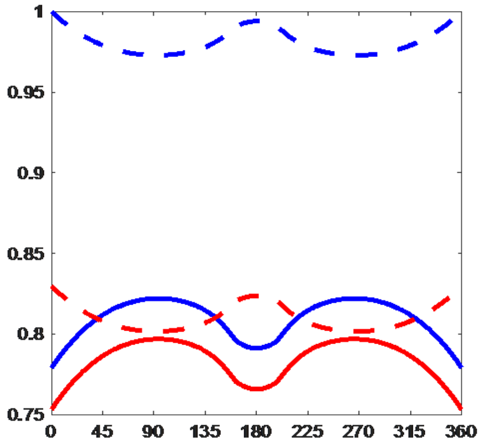

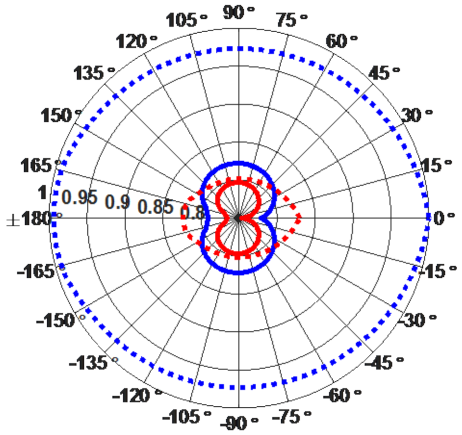

legend

- PP HTI Refl. from top
- PPPP HTI Refl. from bottom
- PP Ortho. Refl. from top
- PPPP Ortho. Refl. from bottom

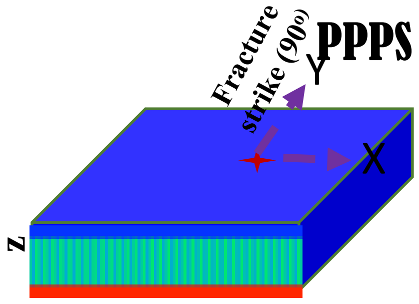

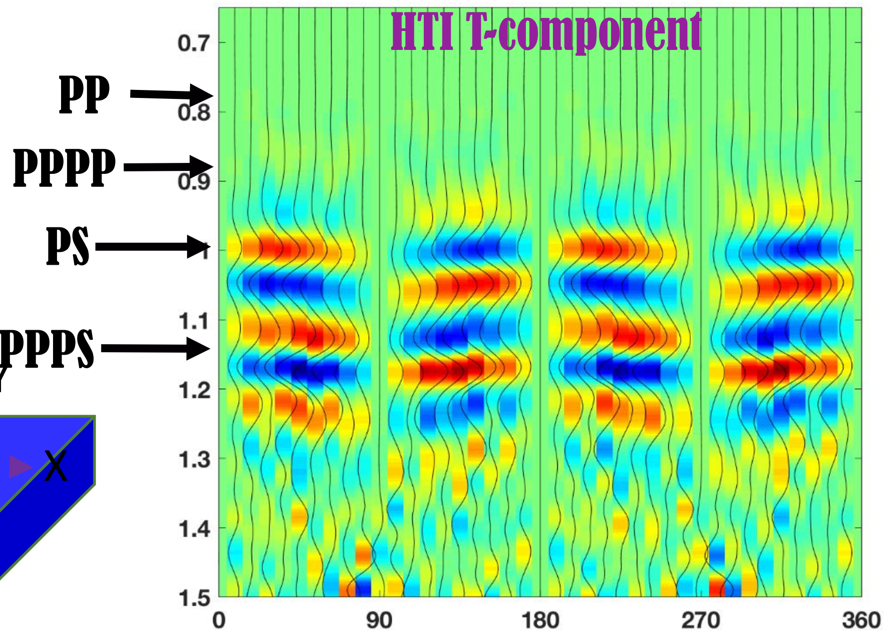

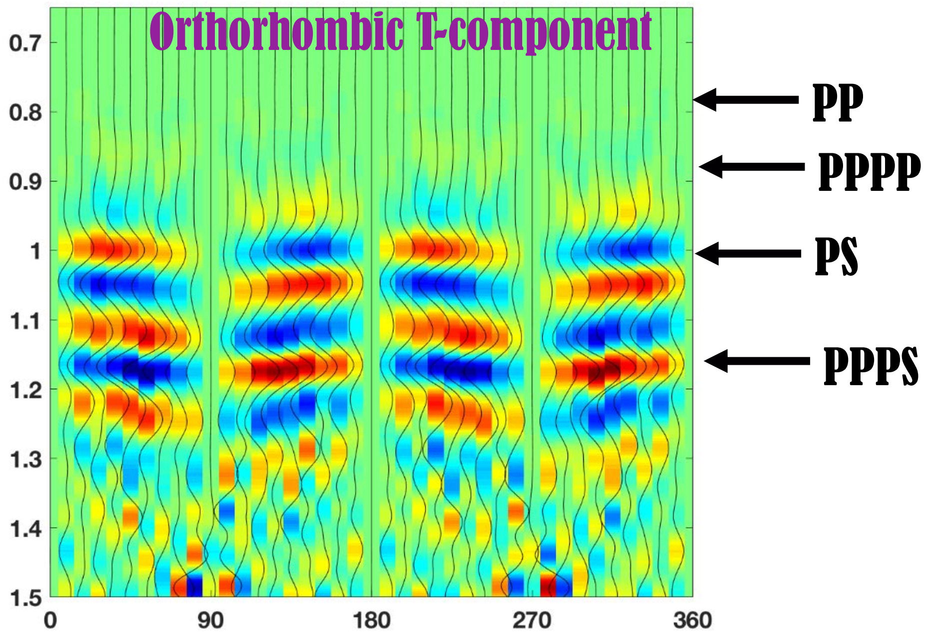

VTI background has no effect on PP reflections.

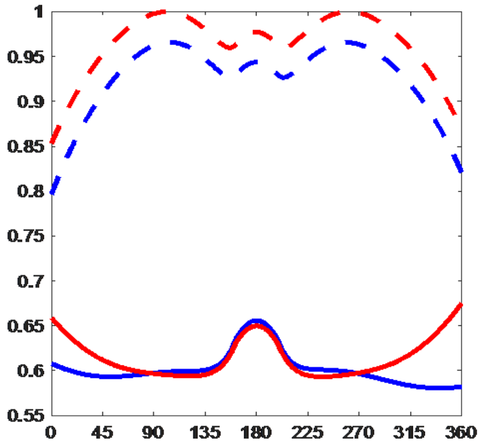

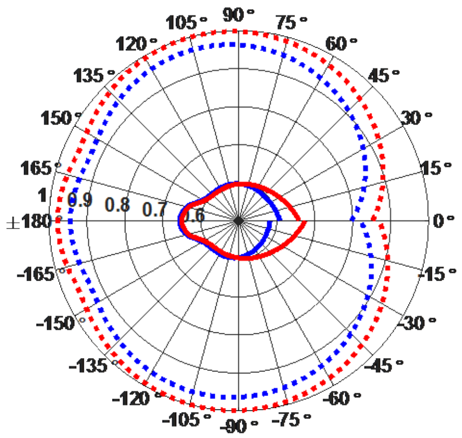

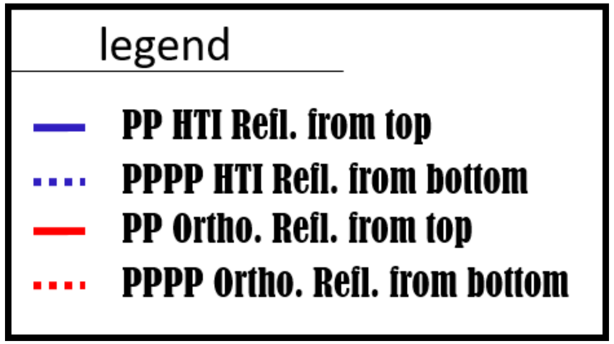

- *Typical orthorhombic modeling of shale reservoir requires at least a VTi/HTI, VTI/TTI, HTI/HTI or a VTI/Orthorhombic models.*

- *We have calculated seismic AVAZ responses in anisotropic shales orthorhombic model based on the finite difference method*

- *Our study shows that the presence of a VTI background affects the PSv converted wave modes and not the quasi PP and quasi P-Sh model*

- *3D elastic finite difference modeling creates numerical issues. Shear wave birefringence may easily be masked by strong artificial boundary reflections.*

- *Although, modeling codes are a means to an end, the modeling technique that best preserves the split-shear waves will be most desired in the future work*

Future work will include looking at the AVAZ responses of this types of orthorhombic models and other combinations and to solve the inverse problem of estimating fracture properties from these datasets.

NSERC, grant CRDPJ 379744-08

CREWES sponsors

Colleagues at CREWES

SINTEF

Thank you for listening

Questions